Why Are a 3 Ions Rarely Observed?

ARTICLE *in* JOURNAL OF THE AMERICAN SOCIETY FOR MASS SPECTROMETRY · JANUARY 2008

Impact Factor: 2.95

7 AUTHORS, INCLUDING:

Benjamin J. Bythell
University of Missouri - St. Louis

Why Are a_3 Ions Rarely Observed?

Julia M. Allen,[a] Alawee H. Racine,[a] Ashley M. Berman,[a] Jeffrey S. Johnson,[a] Benjamin J. Bythell,[b] Béla Paizs,[b] and Gary L. Glish[a]

[a] Department of Chemistry, University of North Carolina, Chapel Hill, North Carolina, USA
[b] German Cancer Research Center, Heidelberg, Germany

It has been determined experimentally that a_3 ions are generally not observed in the tandem mass spectroscopic (MS/MS) spectra of b_3 ions. This is in contrast to other b_n ions, which often have the corresponding a_n ion as the base peak in their MS/MS spectra. Although this might suggest a different structure for b_3 ions compared to that of other b_n ions, theoretical calculations indicate the conventional oxazolone structure to be the lowest energy structure for the b_3 ion of AAAAR, as it is for other b_n ions of this peptide. However, it has been determined theoretically that the a_3 ion is lower in energy than other a_n ions, relative to the corresponding b ions. Furthermore, the $a_3 \rightarrow b_2$ transition structure (TS) is lower in energy than other $a_n \rightarrow b_{n-1}$ TSs of AAAAR, compared with the corresponding b ions. Consequently, it is suggested that the b_3 ion does fragment to the a_3 ion, but that the a_3 ion then immediately fragments (to b_2 and a_3*) because of the excess internal energy arising from its relatively low energy and the facile $a_3 \rightarrow b_2$ reaction. That is why a_3 ions are not observed in the MS/MS spectra of b_3 ions. (J Am Soc Mass Spectrom 2008, 19, 1764–1770) © 2008 American Society for Mass Spectrometry

Tandem mass spectrometry (MS/MS) is by far the most common method for identifying peptides and proteins. Characteristic fragmentations occur along the polypeptide backbone, depending on the ion activation method used. "Slow heating" techniques, such as low-energy collision-induced-dissociation (CID) and infrared multiphoton dissociation (IRMPD), typically cause cleavage at the peptide bond forming b, a, and y ions [1, 2]. Conversely, electron capture dissociation (ECD) cleaves the N—C$_\alpha$ bond to form c and z ions [3, 4]. There is a long history of studying the mechanisms of dissociation of peptide ions, originally concentrating on formation of b-, a-, and y-type ions, [2, 5–17] but more recently the formation of c and z ions [18–22].

It has been shown that significant rearrangement can occur upon peptide dissociation, particularly in mass spectrometers with relatively long activation/dissociation times such as ion trapping instruments [23–28]. However, rearrangements are not limited to ion trapping mass spectrometers [29–32]. In actuality even b and y ions are formed by rearrangements involving hydrogen atom transfers (y ions) or intramolecular cyclization (b ions). The ubiquitousness of the mechanism for formation of b and y ions has been shown through kinetic energy loss measurements [33].

Initially it was thought that b ions had a simple acylium ion structure [5, 34, 35]. However, this theory was discredited because b_1 ions are not often observed in MS/MS spectra (i.e., these ions should also be acylium ions by the preceding rationale). The current consensus is that b ions most commonly have a protonated oxazolone structure [36–39]. This has been demonstrated in gas-phase IR studies on the b_4 ions of YGGFL [38, 40]. Additionally, recent experimental and theoretical data suggest that larger oxazolones can undergo head-to-tail cyclization to form cyclic-peptide isomers [32, 40]. Further evidence supporting the conclusion that b ions have the protonated oxazolone structure is that the major dissociation products of b ions (a_n and b_{n-1} ions) have product ion analogs in the MS/MS spectra of synthesized oxazolone compounds [37].

Although formation of a_n ions via the $b_n \rightarrow a_n$ pathway is well understood [41], the actual mechanism of b_{n-1} formation is less clear. Two major mechanisms were considered here, the direct $b_n \rightarrow b_{n-1}$ [36] and indirect $b_n \rightarrow a_n \rightarrow b_{n-1}$ [42] pathways. Metastable ion studies indicate that a_n ions are formed with substantial release of kinetic energy (KER). On the other hand b_{n-1} fragments are formed from b_n parents with small KER values [36, 37]. This finding suggests that a direct $b_n \rightarrow b_{n-1}$ mechanism is preferred. Additionally, double-resonance experiments in a quadrupole ion trap have been used to study the same reaction [43]. By ejecting the a_4 fragments as they are formed, it was shown that 50% of the b_3 ions of various Leu-enkephalin derivatives are originated directly from the corresponding b_4 ions. Note, however, that both of these experiments have a characteristic time window (microsecond or longer). Practically this means that these techniques provide useful mechanistic information only on reactions of the a_n species if the competing mechanisms result in the transient a_n species having a sufficiently long life-time.

Address reprint requests to Dr. Béla Paizs, German Cancer Research Institute, Department of Molecular Physics, Im Neuenheimer Feld 580, D-69120 Heidelberg, Germany, or Gary L. Glish, University of North Carolina–Chapel Hill, Department of Chemistry, CB# 3290, Chapel Hill, NC 27599-3290. E-mail: b.paizs@dkfz.de or glish@unc.edu

1044-0305/08/$32.00
doi:10.1016/j.jasms.2008.09.022

Published online September 30, 2008
Received July 18, 2008
Revised September 12, 2008
Accepted September 12, 2008

Although the structure and reactivity of *a* ions have received comparatively less attention, both linear and cyclic isomers have been reported [2, 40–45]. Note however, that these studies dealt with b_2 (a_2), b_4 (a_4), and larger b_n ions, and the structure and reactivity of b_3 (a_3) fragments received surprisingly limited attention. The related chemistry shows, however, rather unique features that will be investigated in the present study using a combined experimental and theoretical strategy.

Experimental

An Esquire quadrupole ion trap mass spectrometer (Bruker Daltonics, Billerica, MA, USA) was used for the experiments described herein. Ions were generated via nanoelectrospray ionization, using a capillary voltage of about 1100 V. After the ions were injected into the ion trap, the parent ion, $[M + H]^+$, was isolated. After isolation of the parent ion, collision-induced dissociation (CID) was performed using He as the target gas. The parent ion was resonantly excited via application of a supplemental ac voltage to the end cap electrode. For MS^3 experiments a b_n from the product ions produced in the MS/MS spectrum was isolated and subsequently dissociated using CID.

MS/MS and MS^3 spectra were obtained for 29 different peptides: FLLVPLG, YVGFL, YGVFL, YGWFL, YGPFL, YAAFL, YGGFL, YGGFM, FGGFL, FGGYL, YGAFL, YAGFL, YLGFL, YGLFL, YGGFLRR, RPPGFSPF, PPGFSP, TLGIVCPI, AAAAR, GFAD, WHWLQL, VGVAPG, FLEEI, GGYR, FFFFF, DLWQK, RRPYIL, RYLPT, and VHLTP. The peptide solutions were 75% methanol/20% water/5% acetic acid. The concentration of these samples was 100 μM.

Synthesis of 2-Phenyl-5-oxazolone

2-Phenyl-5-oxazolone was synthesized in accordance with an established procedure, using hippuric acid as the starting material and acetic anhydride as the solvent [46]. The structure of the oxazolone standard was confirmed using ^{1}H NMR and mass spectrometry. ^{1}H NMR (400 MHz, $CDCl_3$, 298 K) revealed δ 4.409 (s, 2H, NCH_2CO), 7.473 (t, 2H, J = 8.0 Hz, *meta*-H), 7.551 (t, 1H, J = 6 Hz, *para*-H), and 7.977 (d, 2H, J = 7.6 Hz, *ortho*-H). This spectrum is consistent with that previously published [47]. The ESI mass spectrum showed only the protonated molecule at *m/z* 162.

Computations

The potential energy surfaces (PES) of the b_2 (AA_{oxa}), b_3 (AAA_{oxa}), and b_4 ($AAAA_{oxa}$) ions derived from the peptide AAAAR were investigated using the strategy developed recently to deal with protonated peptides [2, 13, 45]. These calculations began with molecular dynamics simulations using the Insight II program (Biosym Technologies, San Diego, CA, USA) in conjunction with the AMBER force field [48], modified in-house to enable the study of C-terminal oxazolone and imine groups and $b_n \rightarrow a_n$ and the $a_n \rightarrow b_{n-1}$ transition structures (TS). During the dynamics calculations we used simulated annealing techniques to produce candidate structures for further refinement, applying full geometry optimization using the AMBER force field. These optimized structures were analyzed by a conformer family search program developed in-house. This program groups optimized structures into families for which the most important characteristic torsion angles of the molecule are similar. The most stable species in the families were then fully optimized at the PM3, HF/3-21G, B3LYP/6-31G(d), and finally at the B3LYP/6-31+G(d,p) levels and the conformer families were regenerated at each level. The Gaussian set of programs [49] was used for all ab initio and density functional theory calculations.

For the energetically most preferred structures we performed frequency calculations at the B3LYP/6-31G(d) level of theory. The relative energies were calculated by correcting the B3LYP/6-31+G(d,p) total energies for zero-point vibrational energy (ZPE) and/or thermal and entropy contributions determined from the unscaled B3LYP/6-31G(d) frequencies. For all studied *b* ion PESs the energetically most favored b_n structure is used as the zero energy point on the relative energy scale.

Results and Discussion

MS^3 Experiments

MS^n was used to test the hypothesis that a_n ions form via the consecutive dissociation of b_n ions. In the MS^3 spectra of b_n ions, it is typically observed that b_n ions dissociate to form the corresponding a_n ion as the most intense product ion peak, illustrating that b_n ion dissociation is an efficient method for generating a_n ions. As an example Figure 1 shows the MS^3 spectra of the b_2 and b_4 ions of AAAAR. The b_2 ion from MS/MS of the protonated peptide dissociates almost exclusively to

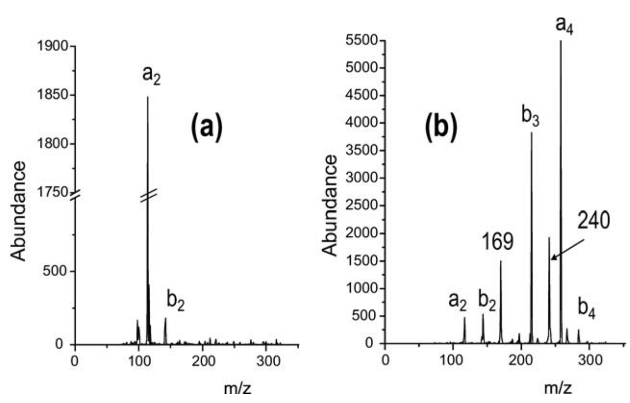

Figure 1. (**a**) MS^3 spectra of the b_2 ion of AAAAR, showing that the a_2 ion is the most intense product ion. (**b**) MS^3 spectra of the b_4 ion of AAAAR, illustrating that the a_4 ion is the most abundant product ion.

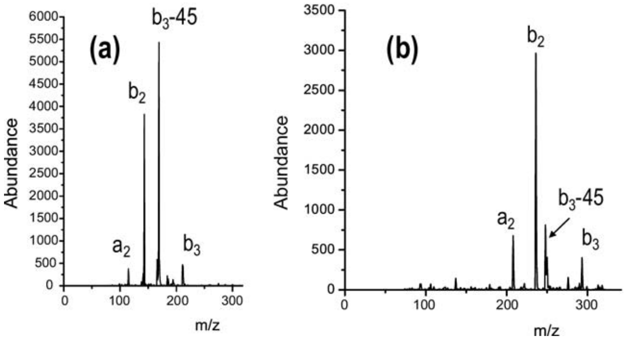

Figure 2. MS^3 spectra of the b_3 ion (**a**) of AAAAR and (**b**) of YAGFL.

form the a_2 ion (Figure 1a) and the b_4 ion of the protonated peptide dissociates to form the a_4 ion as the base peak and lower mass *a* a and *b* ions (Figure 1b). Notably though, whereas a_4, b_3, b_2, and a_2 ions are observed in the spectrum in Figure 1b there is no a_3 ion observed.

Given that the a_n ion is usually formed via dissociation of the corresponding b_n ion, the result in Figure 1b suggests that in this case b_3 does not fragment to form the a_3 ion or that the resulting a_3 ion is unstable with respect to subsequent fragmentation. This is supported by the MS^3 spectrum of the b_3 ion of AAAAR shown in Figure 2a. No large a_3 ion peak was observed in the MS^3 spectra of the b_3 ions. Instead, the b_3 ions dissociated to form b_3-45 (a_3* or a_3-NH_3) as the base peak along with intense b_2 and a_2 peaks. Shown in Figure 2b is the MS^3 spectrum of another typical b_3 ion (derived from YAGFL MS/MS spectrum), in which the b_2 ion is the base peak and the b_3-45 (a_3* or a_3-NH_3) and a_2 peaks are also observed.

This dissociation-pattern discrepancy among b_n ions potentially contradicts the conventional notion that all b_n ions lose CO to form a_n ions. Of the 29 peptides that were used in this work, only two, PPGFSP and RYLPT, had a significant intensity for a_3 ions in the MS/MS spectrum of b_3. Some peptides had a very small amount of a_3 ions in the MS/MS spectrum of b_3 (e.g., AAAAR in Figure 2 has <2% relative intensity of a_3).

In a further investigation, MS/MS was performed on 2-phenyl-5-oxazolone [36]. Since b_n ions are classically thought to have a protonated oxazolone ring on their C-terminal end, they should exhibit similar dissociation pathways as that of 2-phenyl-5-oxazolone. The MS/MS spectrum of 2-phenyl-5-oxazolone contains two product ions, *m/z* 134 and *m/z* 105. The *m/z* 134 product ion corresponds to $[M - CO]^+$, which parallels the loss of CO that accompanies the dissociation pathway of a b_n ion to form the corresponding a_n ion. Since most of the b_n ions studied dissociated to form corresponding a_n ions, this dissociation pathway supports the idea that fragmenting b_n ions indeed have the protonated oxazolone structure. The *m/z* 105 product ion, $[PhCO]^+$, in the 2-phenyl-5-oxazolone MS/MS spectra parallels the loss of the *n*th residue from a b_n ion to form a b_{n-1} ion. The $b_n \rightarrow b_{n-1}$ dissociation pathway is observed in almost all of the MS^3 spectra of b_n ions, including the b_3 ion spectra. The observation that most b_n ions follow similar dissociation pathways as the oxazolone compound ($b_n \rightarrow b_{n-1}$ and $b_n \rightarrow a_n$) strongly supports the proposal that *b* ions have the protonated oxazolone structure [36] or other *b* isomers (like the cyclic-peptide form [32] fragment through oxazolone structures.

Thus, the key discrepancy in the MS/MS spectra of the b_3 ions is that they generally do not have a_3 ions. One possible explanation for the difference in behavior of the b_3 ions relative to other b_n ions is that b_3 has a different structure. Alternatively, the potential energy surface for the dissociation of b_3 might be different from that for other b_n ions. To address these possibilities, ab initio calculations were performed to determine theoretically the energetics of various possible b_2, b_3, b_4, a_2, a_3, and a_4 structures for the AAAAR peptide and also reaction pathways for the dissociation of these ions.

Theoretical calculations

The *b* and *a* ions of peptides consisting of only aliphatic amino acid residues can have linear [36, 37] or cyclic [32, 40] structures. The linear structures are terminated at the C-terminus with oxazolone or imine groups for *b* and *a* ions, respectively. The cyclic *b* isomers can be formed from the oxazolone structures by nucleophilic attack of the N-terminal amino group on the carbonyl carbon of the oxazolone ring [32]. Linear *a* ions can cyclize by nucleophilic attack of the N-terminal amino group on the C-terminal imine carbon [40]. All these structures, including the likely protonation forms, were calculated for the b_4, b_3, b_2, a_4, a_3, and a_2, fragments of AAAAR and the theoretical data are summarized in Schemes 1–3 and Figure 3 (and Figures S1–S6 of the

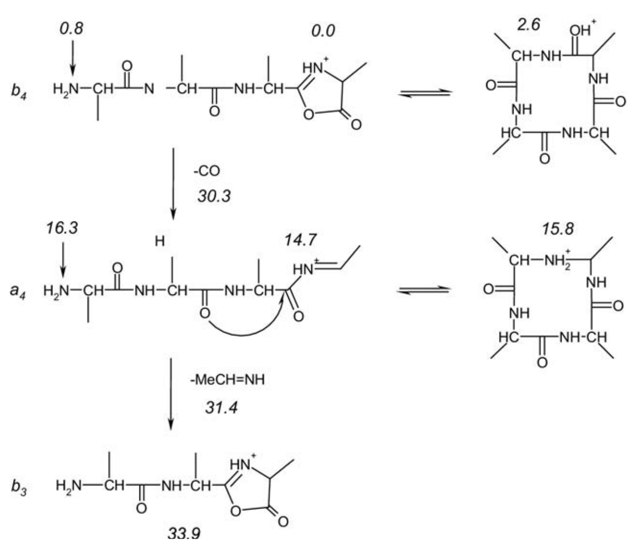

Scheme 1. Structures and relative energies on the b_4 PES (relative energies are in kcal mol^{-1}). Arrows indicate alternative protonation sites.

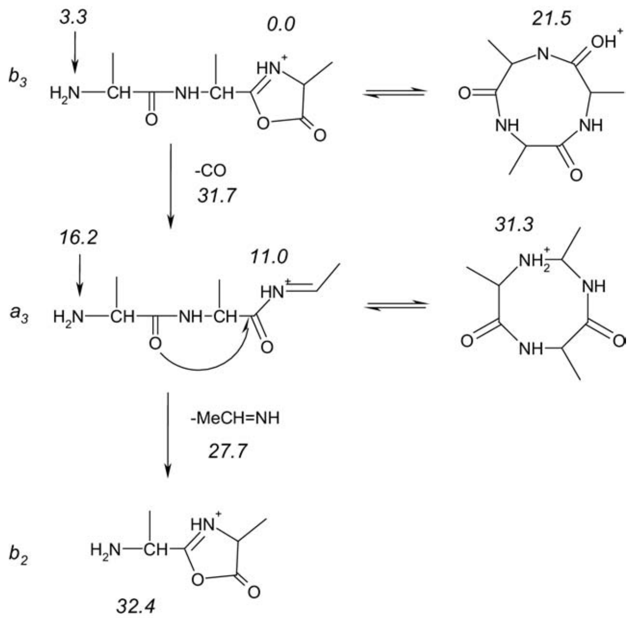

Scheme 2. Structures and relative energies on the b_3 PES (relative energies are in kcal mol^{-1}). Arrows indicate alternative protonation sites.

supplementary material, which can be found in the electronic version of this article).

Two major types of structures were considered for the b_4 fragment of AAAAR, the AAAA$_{\text{oxa}}$ linear and cyclo-(AAAA) macro-cyclic isomers. Similarly to YGGFL [40] the latter is less stable (2.6 kcal mol^{-1}) than the former. This suggests that the majority of the b_4 ion population is present as the oxazolone form in the mass spectrometer. The oxazolone structure has two competing protonation sites: the N-terminal amino and C-terminal oxazolone groups. For AAAA$_{\text{oxa}}$ the latter is slightly favored over the former (Scheme 1).

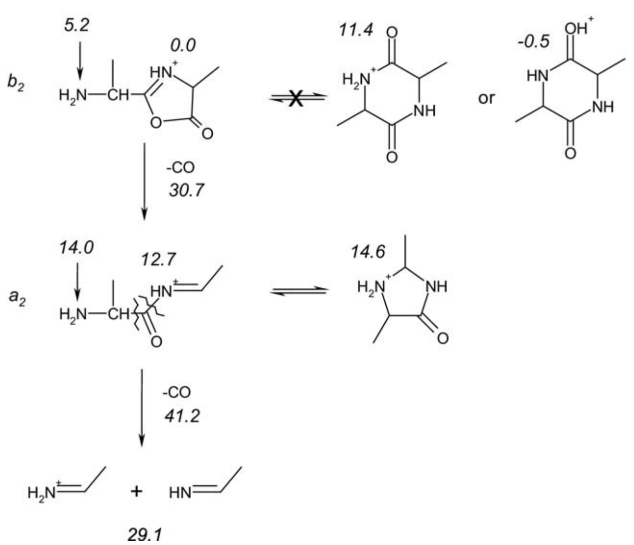

Scheme 3. Structures and relative energies on the b_2 PES (relative energies are in kcal mol^{-1}). Arrows indicate alternative protonation sites.

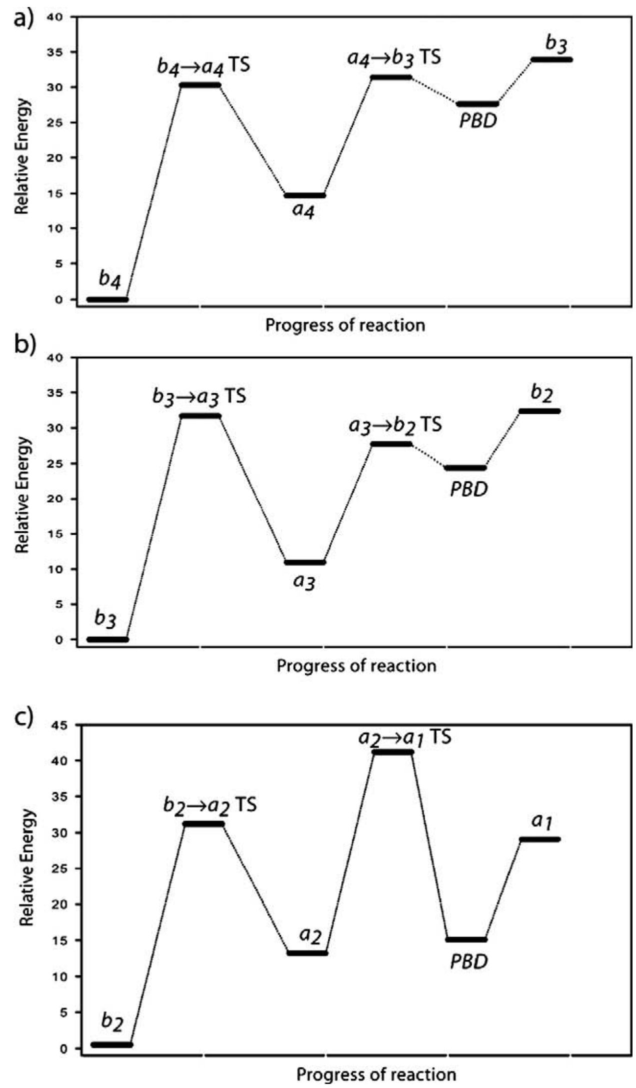

Figure 3. Relative energy level diagrams for the fragment ions of (**a**) b_4, (**b**) b_3, and (**c**) b_2 of [AAAAR + H]$^+$. Relative energies are in kcal mol^{-1}.

The a_4 ions are formed from the oxazolone b_4 isomer via the $b_4 \rightarrow a_4$ CO-loss [41] transition structure at 30.3 kcal mol^{-1} relative energy (calculated with respect to the energetically most favored AAAA$_{\text{oxa}}$ isomer, Scheme 1). On the product wing of this transition structure one finds a loosely bound complex of a_4 and CO which dissociates rather easily leaving the linear a_4 isomer with the protonated C-terminal imine group (14.7 kcal mol^{-1} relative energy) behind. Other, energetically less favored a_4 isomers include the N-terminal protonated linear (16.3 kcal mol^{-1} relative energy) and cyclic (15.8 kcal mol^{-1} relative energy) forms (Scheme 1). These energetics suggest that the majority of the a_4 ion population is present as the C-terminal imine protonated form in the mass spectrometer. This isomer can react by nucleophilic attack of the A(2)–A(3) amide oxygen on the C-terminal amide carbon to form a new oxazolone ring (Scheme 1). This $a_4 \rightarrow b_3$ reaction leads to a proton-bound dimer of b_3 and the former C-terminal imine [28].

Our calculations indicate that the relative energy of the $a_4 \rightarrow b_3$ TS (31.4 kcal mol^{-1}) is only slightly above (Figure 3a) that of the $b_4 \rightarrow a_4$ TS (30.3 kcal mol^{-1}). Furthermore, the energy level (33.9 kcal mol^{-1}) of the final products (b_3, CO, and HN=CHMe) of the reaction cascade of Scheme 1 is also close to the threshold energies of the $a_4 \rightarrow b_3$ and $b_4 \rightarrow a_4$ TSs (Figure 3). The reaction cascade of Scheme 1 with the corresponding energetics (Figure 3a) reasonably explains the experimental MS/MS spectrum (Figure 1b) of the b_4 ion of AAAAR. The less energized fragmenting b_4 species can be trapped and observed as a_4 ions. It should be noted that formation of a ions from b fragments is accompanied by significant kinetic energy release as measured in sector instruments [36, 37]. This means that a large part of the internal energy of fragmenting b fragments is transferred to kinetic energy leading to less energized (i.e., more stable) a ions. However, the a_4 ions formed from the more energized b_4 ions fragment further on the $a_4 \rightarrow b_3$ pathway to form b_3 fragments. The lifetime of these reactive a_4 species is likely to be very short, even shorter than the microsecond time window of the metastable ion and double-resonance experiments used to investigate the mechanism of the $b_n \rightarrow b_{n-1}$ reaction. This means that the conclusions drawn from these experiments should be considered carefully, and that likely this reaction occurs on the indirect $b_n \rightarrow a_n \rightarrow b_{n-1}$ [42] pathways rather than via the direct $b_n \rightarrow b_{n-1}$ [36] mechanism. Overall, the b_4 to b_3 reaction requires approximately 34 kcal mol^{-1} energy to proceed.

The PES of the b_3 fragment (Scheme 2) significantly differs from that of b_4. The linear oxazolone terminated isomer is energetically much more favored than the cyclic peptide structure. This is attributed to the strained nine-membered ring that has to accommodate three amide bonds from which two must be in the *trans* isomerization state (the third amide bond that is introduced by the ring formation can be either *cis* or *trans*). These energetics suggest that the cyclic b_3 can be ruled out as an alternative isomer responsible for the anomalous a_3 fragment abundances observed experimentally.

The a_3 ions are formed from the oxazolone b_3 isomer via the $b_3 \rightarrow a_3$ CO-loss transition structure at 31.7 kcal mol^{-1} relative energy. This reaction has a very similar threshold energy to that of the $b_4 \rightarrow a_4$ pathway (30.3 kcal mol^{-1}). The most favored a_3 isomer is the imine protonated linear form at 11.0 kcal mol^{-1} relative energy. This structure is comparatively lower in energy than the corresponding a_4 isomer (14.7 kcal mol^{-1}). The cyclic a_3 isomer has to accommodate two *trans* or a *trans* and *cis* amide bonds in an eight-membered ring [40]. This results in a very strained structure and a relative energy at 31.3 kcal mol^{-1}.

The imine protonated a_3 isomer fragments further to produce the b_2 ion via the $a_3 \rightarrow b_2$ TS at 27.7 kcal mol^{-1} relative energy (Scheme 2, Figure 4). The $a_4 \rightarrow b_3$ TS has a significantly higher relative energy at 31.4 kcal mol^{-1}.

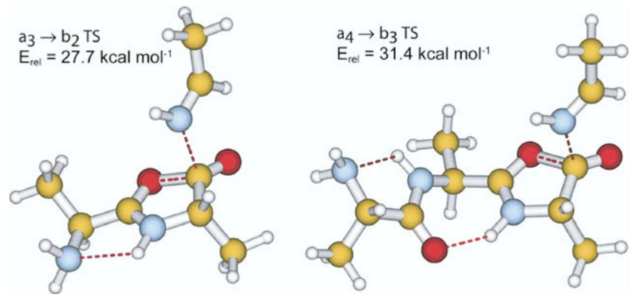

Figure 4. The $a_3 \rightarrow b_2$ and the $a_4 \rightarrow b_3$ TSs with relative energies (kcal mol^{-1}).

The structural differences between the $a_3 \rightarrow b_2$ and the $a_4 \rightarrow b_3$ TSs are small and why such small changes should result in these energy differences is not entirely clear. However, both TSs result in the most stable corresponding b_n ion being formed and were generated from extensive PES searches. The $a_3 \rightarrow b_2$ TS is also lower in energy than the $b_3 \rightarrow a_3$ TS, which produces the a_3 population (Figure 3b). Consequently, these a_3 ions are transient species that fragment further immediately after their formation so are not observed upon CID of b_3. The energy level (32.4 kcal mol^{-1}) of the final products (b_2, CO, and HN=CHMe) of the reaction cascade of Scheme 2 is slightly above that of the $b_3 \rightarrow a_3$ threshold energy (Figure 3b). Thus the small peak corresponding to the *m/z* of the a_3 ion is most likely an undissociated proton-bound dimer of the b_2 ion and HN=CHMe rather than the transient a_3 ion itself. This phenomenon also explains the abundant a_3 observed in the metastable ion spectrum of AAA$_{oxa}$ by Harrison and coworkers [36].

The PES of the b_2 fragment (Scheme 3) differs significantly from those of b_4 and b_3. The oxazolone and cyclic peptide (diketopiperazine derivative) isomers are nearly equienergetic. However, these two isomers have very different structures (single *trans* amide bond for the oxazolone versus two *cis* amide bonds for the diketopiperazine derivative) and they cannot directly interconvert because of the high barrier involved [2, 50].

The a_2 ions are formed from the oxazolone b_2 isomer via the $b_2 \rightarrow a_2$ CO-loss transition structure at 30.7 kcal mol^{-1} relative energy. This TS also has a very similar relative energy to that of the $b_4 \rightarrow a_4$ and $b_3 \rightarrow a_3$ TSs (30.3 and 31.3 kcal mol^{-1}, respectively). The most favored a_2 isomer is the imine protonated linear structure. This species can cyclize to form an energetically only slightly less favored five-membered ring that accommodates a *cis* amide bond. This reaction is facilitated by the reduced partial double-bond character of this amide bond in the linear imine protonated structure [40].

The a_2 ions can fragment further by expulsion of CO via cleavages of the C$_\alpha$—CO and OC—N bonds [45]. This reaction leads to the proton bound homo-dimer of HN=CHMe via the $a_2 \rightarrow a_1$ TS at 41.2 kcal mol^{-1} relative energy. This TS is clearly higher in energy than $a_4 \rightarrow b_3$

or $a_3 \rightarrow b_2$ (31.4 or 27.7 kcal mol^{-1}, respectively). This barrier provides the a_2 fragment extra stability, in agreement with our experimental data, which show very limited fragmentation of this species (Figure 1b).

Conclusion

Experimentally most b_3 ions do not appear to form a_3 ions, in contrast to other b_n ions, which readily lose CO to form the corresponding a_n ion. This suggests that b_3 ions have a unique structure compared to other b_n ions or there is some barrier to the loss of CO or the a_3 ion is less stable than other a_n fragments. Theoretical calculations on the possible structures of b_3 of AAAAR indicate that the conventional oxazolone structure is the lowest energy form. The calculations also indicate that the relative energy of the a_3 ion is lower than that of other a_n ions. This very stability enables subsequent fragmentation of the a_3 ion without the need for any additional energy to be acquired as the $a_3 \rightarrow b_2$ transition structure is lower in energy than the preceding $b_3 \rightarrow a_3$ transition structure. Furthermore, the $a_3 \rightarrow b_2$ transition structure is lower in energy than other $a_n \rightarrow b_{n-1}$ TSs of AAAAR, so b_3 ions do indeed form a_3 ions, but the a_3 ions undergo further fragmentation on a timescale faster than can be observed in a quadrupole ion trap. Such fast consecutive dissociations in a quadrupole ion trap for similar type ions has been reported previously [51]. The calculated energetics of the $b_4 \rightarrow a_4 \rightarrow b_3 \rightarrow a_3 \rightarrow b_2 \rightarrow a_2 \rightarrow a_1$ reaction cascade clearly explains our CID data observed for the b_n fragments of the AAAAR model peptide. Our calculations on the PES of YGGFL fragments (B. Paizs, unpublished data) indicate the same tendency. To assess the general validity of these observations further theoretical studies on a number of model peptides are needed.

References

1. Biemann, K. Contributions of Mass Spectrometry to Peptide and Protein Structure. *Biomed. Environ. Mass Spectrom.* **1988,** *16,* 99–111.
2. Paizs, B.; Suhai, S. Fragmentation Pathways of Protonated Peptides. *Mass Spectrom. Rev.* **2004,** *24,* 508–548.
3. Zubarev, R. A. Reactions of Polypeptide Ions with Electrons in the Gas Phase. *Mass Spectrom. Rev.* **2003,** *22,* 57–77.
4. Zubarev, R. A.; Zubarev, A. R.; Savitski, M. M. Electron Capture/Transfer versus Collisionally Activated/Induced Dissociations: Solo or Duet? *J. Am. Soc. Mass Spectrom.* **2008,** *19,* 753–761.
5. Hunt, D. F.; Yates, J. R., 3rd; Shabanonowitz, J.; Winston, S.; Hauer, C. R. Protein Sequencing by Tandem Mass Spectrometry. *Proc. Natl. Acad. Sci. U. S. A.* **1986,** *83,* 6233–6237.
6. Johnson, R. S.; Martin, S. A.; Biemann, K.; Stults, J. T.; Watson, J. T. Novel Fragmentation Process of Peptides by Collision-Induced Decomposition in a Tandem Mass Spectrometer: Differentiation of Leucine and Isoleucine. *Anal. Chem.* **1987,** *59,* 2621–2625.
7. Thorne, G. C.; Gaskell, S. J. Elucidation of Some Fragmentations of Small Peptides Using Sequential Mass Spectrometry on a Hybrid Instrument. *Rapid Commun. Mass Spectrom.* **1989,** *3,* 217–221.
8. McCormack, A. L.; Somogyi, A.; Dongré, A. R.; Wysocki, V. H. Fragmentation of Protonated Peptides: Surface-Induced Dissociation in Conjunction with a Quantum Mechanical Approach. *Anal. Chem.* **1993,** *65,* 2859–2872.
9. Dongré, A. R.; Somogyi, Á.; Wysocki, V. H. Surface-Induced Dissociation: An Effective Tool to Probe Structure, Energetics and Fragmentation Mechanisms of Protonated Peptides. *J. Mass Spectrom.* **1996,** *31,* 339–350.
10. Vaisar, T.; Urban, J. Probing the Proline Effect in CID of Protonated Peptides. *J. Mass Spectrom.* **1996,** *31,* 1185–1187.
11. Dongré, A. R.; Jones, J. L.; Somogyi, Á.; Wysocki, V. H. Influence of Peptide Composition, Gas-Phase Basicity, and Chemical Modification on Fragmentation Efficiency: Evidence for the Mobile Proton Model. *J. Am. Chem. Soc.* **1996,** *118,* 8365–8374.
12. Polce, M. J.; Ren, D.; Wesdemiotis, C. Dissociation of the Peptide Bond in Protonated Peptides. *J. Mass Spectrom.* **2000,** *35,* 1391–1398.
13. Paizs, B.; Suhai, S. Towards Understanding the Tandem Mass Spectra of Protonated Oligopeptides. 1: Mechanism of Amide Bond Cleavage. *J. Am. Soc. Mass Spectrom.* **2004,** *15,* 103–113.
14. Paizs, B.; Lendvay, G.; Vékey, K.; Suhai, S. Formation of b2+ Ions from Protonated Peptides: An Ab Initio Study. *Rapid Commun. Mass Spectrom.* **1999,** *13,* 525–533.
15. Paizs, B.; Suhai, S.; Harrison, A. G. Experimental and Theoretical Investigation of the Main Fragmentation Pathways of Protonated H-Gly-Gly-Sar-Oh and H-Gly-Sar-Sar-Oh. *J. Am. Soc. Mass Spectrom.* **2003,** *14,* 1454–1469.
16. Laskin, J.; Bailey, T. H.; Futrell, J. H. Mechanisms of Peptide Fragmentation from Time- and Energy-Resolved Surface-Induced Dissociation Studies: Dissociation of Angiotensin Analogs. *Int. J. Mass Spectrom.* **2006,** *249,* 462–472.
17. Farrugia, J. M.; O'Hair, R. A. J.; Reid, G. E. Do All b2 Ions Have Oxazolone Structures? Multistage Mass Spectrometry and Ab Initio Studies on Protonated N-Acyl Amino Acid Methyl Ester Model Systems. *Int. J. Mass Spectrom.* **2001,** *210–211,* 71–87.
18. Zubarev, R. A.; Haselmann, K. F.; Budnik, B.; Kjeldsen, F. Jensen, F. Towards an Understanding of the Mechanism of Electron-Capture Dissociation: A Historical Perspective and Modern Ideas. *Eur. J. Mass Spectrom.* **2002,** *8,* 337–349.
19. Syrstad, E. A.; Turecek, F. Toward a General Mechanism of Electron Capture Dissociation. *J. Am. Soc. Mass Spectrom.* **2005,** *16,* 208–224.
20. Holm, A. I. S.; Hvelplund, P.; Kadhane, U.; Larsen, M. K.; Liu, B.; Nielsen, S. B.; Panja, S.; Pedersen, J. M.; Skrydstrup, T.; Stochkel, K.; Williams, E. R.; Worm, E. S. On the Mechanism of Electron-Capture-Induced Dissociation of Peptide Dications from 15n-Labeling and Crown-Ether Complexation. *J. Phys. Chem. A.* **2007,** *111,* 9641–9643.
21. Savitski, M. M.; Kjeldsen, F.; Nielsen, M. L.; Zubarev, R. A. Hydrogen Rearrangement to and from Radical Z Fragments in Electron Capture Dissociation of Peptides. *J. Am. Soc. Mass Spectrom.* **2007,** *18,* 113–120.
22. Rand, K. D.; Adams, C. M.; Zubarev, R. A.; Jorgensen, T. J. D. Electron Capture Dissociation Proceeds with a Low Degree of Intramolecular Migration of Peptide Amide Hydrogens. *J. Am. Chem. Soc.* **2008,** *130,* 1341–1349.
23. Vachet, R. W.; Bishop, B. M.; Erickson, B. W.; Glish, G. L. Novel Peptide Dissociation: Gas-Phase Intramolecular Rearrangement of Internal Amino Acid Residues. *J. Am. Chem. Soc.* **1997,** *119,* 5481–5488.
24. Payne, A. H.; Glish, G. L. Thermally Assisted Infrared Multiphoton Photodissociation in a Quadrupole Ion Trap. *Anal. Chem.* **2001,** *73,* 3542–3548.
25. Yague, J.; Paradela, A.; Ramos, M.; Ogueta, S.; Marina, A.; Barahona, F.; de Castro, J. A. L.; Vazquez, J. Peptide Rearrangement During Quadrupole Ion Trap Fragmentation: Added Complexity to MS/MS Spectra. *Anal. Chem.* **2003,** *75,* 1524–1535.
26. Bythell, B. J.; Barofsky, D. F.; Pingitore, F.; Wang, P.; Wesdemiotis, C.; Paizs, B. Backbone Cleavages and Sequential Loss of Carbon Monoxide and Ammonia from Protonated AGG: A Combined Tandem Mass Spectrometry, Isotope Labeling, and Theoretical Study. *J. Am. Soc. Mass Spectrom.* **2007,** *18,* 1291–1303.
27. Olsen, J. V.; Mann, M. Improved Peptide Identification in Proteomics by Two Consecutive Stages of Mass Spectrometric Fragmentation. *Proc. Natl. Acad. Sci. U. S. A.* **2004,** *101,* 13417–13422.
28. Cooper, T.; Talaty, E.; Grove, J.; Suhai, S.; Paizs, B.; Van Stipdonk, M. Isotope Labeling and Theoretical Study of the Formation of a3* Ions from Protonated Tetraglycine. *J. Am. Soc. Mass Spectrom.* **2006,** *17,* 1654–1664.
29. Alexander, A. J.; Thibault, P.; Boyd, R. K. Collision-Induced Dissociations of Peptide Ions. 2. Remote Charge-Site Fragmentations in a Tandem, Hybrid Mass Spectrometer. *Rapid Commun. Mass Spectrom.* **1989,** *3,* 30–34.
30. Thorne, G. C.; Ballard, K. D.; Gaskell, S. J. Metastable Decomposition of Peptide $[M + H]^+$ Ions via Rearrangement Involving Loss of the C-Terminal Amino Acid Residue. *J. Am. Soc. Mass Spectrom.* **1990,** *1,* 249–257.
31. Rakov, V. S.; Borisov, O. V.; Whitehouse, C. M. Establishing Low-Energy Sequential Decomposition Pathways of Leucine Enkephalin and Its N- and C-Terminus Fragments Using Multiple-Resonance Cid in Quadrupolar Ion Guide. *J. Am. Soc. Mass Spectrom.* **2004,** *15,* 1794–1809.
32. Harrison, A. G.; Young, A. B.; Bleiholder, C.; Suhai, S.; Paizs, B. Scrambling of Sequence Information in Collision-Induced Dissociation of Peptides. *J. Am. Chem. Soc.* **2006,** *128,* 10364–10365.
33. Vachet, R. W.; Winders, A. D.; Glish, G. L. Correlation of Kinetic Energy Losses in High-Energy Collision-Induced Dissociation with Observed Peptide Product Ions. *Anal. Chem.* **1996,** *68,* 522–526.
34. Chu, I. K.; Shoeib, T.; Guo, X.; Rodriquez, C. F.; Lau, T.-C.; Hopkinson, A. C.; Siu, K. W. M. Characterization of the Product Ions from the Collision-Induced Dissociation of Argentinated Peptides. *J. Am. Soc. Mass Spectrom.* **2001,** *12,* 163–175.
35. Johnson, R. S.; Martin, S. A.; Biemann, K. Collision-Induced Fragmentation of $(M + H)^+$ Ions of Peptides. Side Chain Specific Sequence Ions. *Int. J. Mass Spectrom. Ion Processes.* **1988,** *86,* 137–154.

36. Yalcin, T.; Csizmadia, I. G.; Peterson, M. R.; Harrison, A. G. The Structure and Fragmentation of b_n ($n \geq 3$) Ions in Peptide Spectra. *J. Am. Soc. Mass Spectrom.* **1996,** *7,* 233–242.
37. Harrison, A. G.; Csizmadia, I. G.; Tang, T.-H. Structure and Fragmentation of b2 Ions in Peptide Mass Spectra. *J. Am. Soc. Mass Spectrom.* **2000,** *11,* 427–436.
38. Polfer, N. C.; Oomens, J.; Suhai, S.; Paizs, B. Spectroscopic and Theoretical Evidence for Oxazolone Ring Formation in Collision Induced Dissociation of Peptides. *J. Am. Chem. Soc.* **2005,** *127,* 17154–17155.
39. Chen, X.; Turecek, F. Simple b-Ions Have Cyclic Structures. A Neutralization-Reionization Mass Spectrometric and Computational Study. *J. Am. Soc. Mass Spectrom.* **2005,** *16,* 1941–1956.
40. Polfer, N. C.; Oomens, J.; Suhai, S.; Paizs, B. Infrared Spectroscopy and Theoretical Studies on Gas-Phase Protonated Leu-enkephalin and Its Fragments: Direct Experimental Evidence for the Mobile Proton. *J. Am. Chem. Soc.* **2007,** *129,* 5887–5897.
41. Paizs, B.; Szlavik, Z.; Lendvay, G.; Vékey, K.; Suhai, S. Formation of a2+ ions of protonated peptides. An Ab Initio Study. *Rapid Commun. Mass Spectrom.* **2000,** *14,* 746–755.
42. Fang, D. C.; Yalcin, T.; Tang, T. H.; Fu, X. Y.; Harrison, A. G.; Csizmadia, I. G. Electron Distribution in Cationic Fragments Generated Mass Spectrometrically from Peptides. *J. Mol. Struct.* (*Theochem.*) **1999,** *468,* 135–149.
43. Vachet, R. W.; Ray, K. L.; Glish, G. L. Origin of Product Ions in the MS/MS Spectra of Peptides in a Quadrupole Ion Trap. *J. Am. Soc. Mass Spectrom.* **1998,** *9,* 341–344.
44. Ambihapathy, K.; Yalcin, T.; Leung, H. W.; Harrison, A. G. Pathways to Immonium Ions in the Fragmentation of Protonated Peptides. *J. Mass Spectrom.* **1997,** *32,* 209–215.
45. Harrison, A.G.; Young, A. B.; Schnölzer, M.; Paizs, B. Formation of Iminium Ions by Fragmentation of a2 Ions. *Rapid Commun. Mass Spectrom.* **2004,** *18,* 1635–1640.
46. Vandenburg, G. E.; Harrison, J. B.; Carter, H. E.; Magerlein, B. J. Synthesis of 2-Phenyl-5-oxazolone. *Org. Synth.* **2002,** *5,* 101.
47. Lee, V. W.; Li, H.; Lau, T.; Siu, K. W. M. Structures of b and a Product Ions from the Fragmentation of Argentinated Peptides. *J. Am. Chem. Soc.* **1998,** *120,* 7302–7309.
48. Case, D. A.; Pearlman, D. A.; Caldwell, J. W.; Cheatham III, T. E.; Ross, W. S.; Simmerling, C. L.; Darden, T. A.; Merz, K. M.; Stanton, R. V.; Cheng, A. L.; Vincent, J. J.; Crowley, M.; Tsui, V.; Radmer, R. J.; Duan, Y.; Pitera, J.; Massova, I. G.; Seibel, G. L.; Singh, U. C.; Weiner, P. K.; Kollmann, P. A. In *AMBER 99*, University of California: San Francisco, 1999.
49. Frisch, M. J.; Trucks, G. W.; Schlegel, H. B.; Scuseria, G. E.; Robb, M. A.; Cheeseman, J. R.; Montgomery, Jr., J. A.; Vreven, T.; Kudin, K. N.; Burant, J. C.; Millam, J. M.; Iyengar, S. S.; Tomasi, J.; Barone, V.; Mennucci, B.; Cossi, M.; Scalmani, G.; Rega, N.; Petersson, G. A.; Nakatsuji, H.; Hada, M.; Ehara, M.; Toyota, K.; Fukuda, R.; Hasegawa, J.; Ishida, M.; Nakajima, T.; Honda, Y.; Kitao, O.; Nakai, H.; Klene, M.; Li, X.; Knox, J. E.; Hratchian, H. P.; Cross, J. B.; Bakken, V.; Adamo, C.; Jaramillo, J.; Gomperts, R.; Stratmann, R. E.; Yazyev, O.; Austin, A. J.; Cammi, R.; Pomelli, C.; Ochterski, J. W.; Ayala, P. Y.; Morokuma, K.; Voth, G. A.; Salvador, P.; Dannenberg, J. J.; Zakrzewski, V. G.; Dapprich, S.; Daniels, A. D.; Strain, M. C.; Farkas, O.; Malick, D. K.; Rabuck, A. D.; Raghavachari, K.; Foresman, J. B.; Ortiz, J. V.; Cui, Q.; Baboul, A. G.; Clifford, S.; Cioslowski, J.; Stefanov, B. B.; Liu, G.; Liashenko, A.; Piskorz, P.; Komaromi, I.; Martin, R. L.; Fox, D. J.; Keith, T.; Al-Laham, M. A.; Peng, C. Y.; Nanayakkara, A.; Challacombe, M.; Gill, P. M. W.; Johnson, B.; Chen, W.; Wong, M. W.; Gonzalez, C.; and Pople, J. A. Gaussian 03, Revision C.02, Gaussian, Inc.: Wallingford, CT, 2004.
50. Paizs, B.; Suhai, S. Combined Quantum Chemical and RRKM Modeling of the Main Fragmentation Pathways of Protonated GGG. I. *Cis-trans* Isomerization around Protonated Amide Bonds. *Rapid Commun. Mass Spectrom.* **2002,** *15,* 2307–2323.
51. Asam, M. R.; Glish, G. L. Determination of the Dissociation Kinetics of a Transient Intermediate. *J. Am. Soc. Mass Spectrom.* **1999,** *10,* 119–125.